



OPEN

Ecological risk and spatial distribution, sources of heavy metals in typical purple soils, southwest China

Cang Gong^{1,2}, Licheng Quan¹✉, Wenbin Chen¹, Guanglong Tian¹, Wei Zhang¹, Fei Xiao¹ & Zhixiang Zhang¹✉

The identification and quantification of the ecological risks, sources and distribution of heavy metals in purple soils are essential for regional pollution control and management. In this study, geo-accumulation index (I_{geo}), enrichment factor (EF), pollution index (PI), potential ecological risk index (RI), principal component analysis (PCA) model and geographical detector (GD) were combined to evaluate the status, ecological risk, and sources of heavy metals (HMs) in soils from a typical purple soil areas of Sichuan province. The results showed that the average contents of As, Cd, Cr, Cu, Hg, Ni, Pb and Zn in purple soil were 7.77, 0.19, 69.5, 27.9, 0.077, 30.9, 26.5 mg/kg and 76.8 mg/kg, and the I_{geo} , EF and RI of topsoil Hg and Cd in designated area was the highest, and the average contents of Hg and Cd in topsoil were obviously greater than respective soil background value in Sichuan province and purple soil. The hot spots for the spatial distribution of 8 HMs were mainly focused in the southwest and northeast of the designated area, and there were also significant differences for 8 HMs distribution characteristics in the profile soil. Cu comes from both anthropogenic and natural sources, Zn, Ni and Cr mainly come from natural sources, but As, Pb, Hg and Cd mainly derived from human activities. GD results showed that soil texture (X_{18}), altitude (X_4), total nitrogen (TN), clay content (X_3), sand content (X_2) and silt content (X_1) had the greatest explanatory power to 8 HMs spatial differentiation. This study provides a reference for understanding the status and influencing factors of HM pollution in typical purple soil, and lays a theoretical foundation for the environmental treatment of purple soil in China.

Keywords Purple soils, Ecological risk, Spatial distribution, Heavy metals, Geographical detector

Soil is a precious natural resources, human survival and agricultural production are inseparable from clean soil. Accompanied by rapid development of agriculture, industrialization and urbanization, the problem of soil pollution has become increasingly prominent^{1,2}. Global soil heavy metal (HM) pollution accidents occur frequently and the form is becoming more and more serious. Soil HM contamination has become one of the serious eco-environmental issues faced by the development of various countries^{3,4}. Soil heavy metals (HMs) accumulated will have a negative impact on soil nutrient cycling⁵ and crop yield and quality⁶. Soil HMs can enter body through skin contact and inhalation⁷ or by the food chain⁸. Generally speaking, in nature, soil HMs mainly come from parent materials of soil⁹, and natural HMs mainly exist in the form that plants are difficult to use, and there is a low ecological risk¹⁰. Human activities, such as agricultural fertilization, industrial activities and vehicle emissions can increase the accumulation of HMs in soil¹¹. Anthropogenic HMs often take high biological activity, are easy to be absorbed and utilized by plants, and have high ecological risks, and aggravate HMs spatial variability in soil. It is the key to effective deal with soil HM pollution, trace its source and explore the factors that affect the spatial differentiation characteristics of soil HMs. Last 10 years, many researches and analysis have been conducted both domestically and internationally on the driving factors of soil HM pollution^{12–17}.

In recent years, the evaluation indexes of soil HM pollution, including factor of enrichment (EF), index of potential ecological risk (RI) and index of geological accumulation (I_{geo}) has been widely applied in practice¹⁸. The method of contaminant source division can be divided into identification of pollution source and quantification

¹Research Center of Applied Geology of China Geological Survey, Chengdu 610039, China. ²Key Laboratory of Natural Resource Coupling Process and Effects, Beijing 100055, China. ✉email: quanlicheng@mail.cgs.gov.cn; zzhixiang@mail.cgs.gov.cn

of pollution source. Pollution source identification is usually calculated by the cluster analysis, principal component analysis¹⁹ and geographic information system²⁰, while the quantification of pollution sources is realized by receptor models, such as positive matrix factorization, balance of chemical mass, and geographic detector, which is extensively used because they can quantitatively display the contribution of different pollution sources in many researches^{4,21–23}. Multivariate statistical analysis, geostatistical models²⁴ and some comprehensive methods have gradually improved the study of the sources and spatial differentiation of HMs in soils. Accordingly, various evaluation indexes were applied to assess soil HM contaminant, such as I_{geo} , EF, RI and pollution index (PI)²⁵.

Purple soil is usually classified as regosol or entisol²⁶. A series of red or purple rocks from the Triassic to Cretaceous period formed the purple soil²⁶. A large amount of this type of soil is distributed in the Sichuan Basin, which is one of the greatest agricultural areas in southwest China. With the serious trouble between the land resources limitation and the population surge, more and more purple soil was used into agricultural soil, and part purple soil was developed for production of intensive agriculture because its rich mineral nutrition. Most of the existing studies focus on the background value, baseline, content²⁷, distribution²⁸ and migration characteristics²⁹ of HMs in purple soil, and there are few studies on the sources, ecological risk and spatial differentiation of HMs in purple soil. In particular, there are few reports on the potential ecological risks and driving factors of HMs in purple soil. This study aims to (1) assess the concentration and pollution levels of HMs in typical purple soils; (2) identify the main sources of HMs in typical purple soils; (3) assess the main drivers of HM pollution in typical purple soils based on the GeoDetector model; and (4) assess the potential ecological risks of HMs in typical purple soils. The research results can provide important theoretical and practical reference for the source identification, risk assessment and comprehensive treatment of HM pollution in purple soil, and will lay a theoretical foundation for environmental management and regional sustainable development of purple soil in China.

Materials and methods

Research area

The research area was situated in the east of Sichuan Province, longitude 105°56'–107°19' E, latitude 30°01'–30°52' N, with an area of 6339 km² and a total population of 4.7 million. The topography of the research area is east high and west low, and the zoning characteristics are obvious. The research area was situated in the humid monsoon climate area of the middle subtropics, with a warm climate, abundant heat and abundant rainfall, an annual average precipitation is 1054.46 mm–1512.45 mm, an annual mean temperature is 16 °C. The territory of 210, 212, 305, 318 national highways and 203, 304, 18 provincial highways and county, township, village roads crisscross, the highway network extends in all directions. The Jialing River and the Qujiang River cross the border.

Sampling and analysis

Field sampling to be completed in 2022. A total of 73 topsoil samples (0–20 cm) were collected according to the specification of land quality geochemical assessment (DZ/T 0295–2016)³⁰. Sampling sites were displayed in Fig. 1. The sampling points were uniformly arranged in a 4 km² sampling grid, and the distance between each sampling point was required to be greater than 2 km. 3–5 multi-point collections within 100 m around the sampling point are combined into one sample, and the original weight of the combined sample is greater than 1 kg. Locate sampling points with portable GPS. 5 profile sampling points PMA, PMB, PMC, PMD and PME in the study area, with a profile depth of 1 m, and one sample is collected for each 20 cm.

C_{org} was measured by volumetric method, N was measured by combustion infrared method, atomic fluorescence method was used measure the content of Hg and As, Cu, Pb, Ni, Zn, Sc, Cr, P, Cd and K were measured by x-ray fluorescence spectroscopy (XRF), inductively coupled plasma mass spectrometry (ICP-MS) and inductively Coupled Plasma Optical Emission Spectrometer (ICP-OES). The quality of analysis and testing was

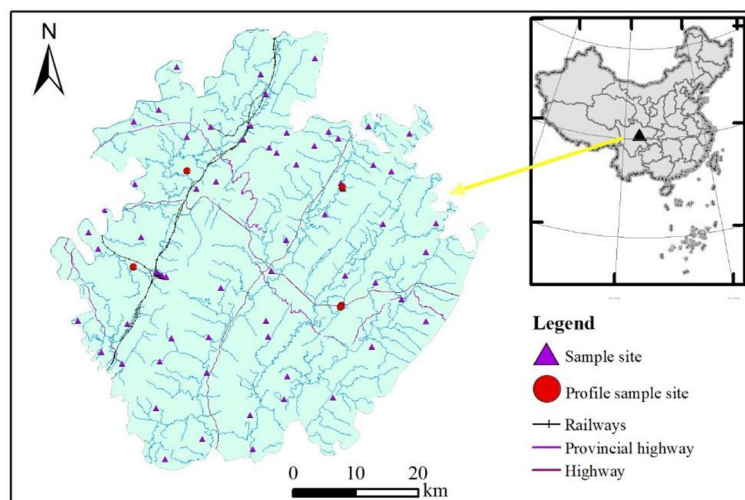


Figure 1. The location of research area and sampling sites.

controlled by means of inserting national first-level soil standard materials, repeatability inspection, abnormal point inspection, and blank test.

Geo-accumulation Index (I_{geo})

The I_{geo} method can be used to compare the concentration of different soil HMs and their pollution degree³¹.

$$I_{\text{geo}} = \log_2 \left(\frac{C_i}{K \times B_i} \right) \quad (1)$$

where I_{geo} was soil accumulation index of HM i ; C_i was measured value of soil HM i ; B_i was guideline value, and background value of profile soil was selected (Table 1); k was the correction coefficient, generally 1.5. The pollution degree of I_{geo} can be divided into seven grades: < 0 (unpolluted), 0–1 (mild contaminated), 1–2 (moderate contaminated), 2–3 (moderate-heavy contaminated), 3–4 (heavy contaminated), 4–5 (heavy-extreme contaminated) and > 5 (extremely heavy contaminated).

Enrichment Factor (EF)

EF was a useful index to distinguish between human activities or natural sources of HMs. EF was calculated³²:

$$EF = [M_i/M_{Sc}]_S / [M_i/M_{Sc}]_B \quad (2)$$

where $[M_i/M_{Sc}]_S$ was the content ratio of HM i to Sc in samples, while $[M_i/M_{Sc}]_B$ was the ratio of purple soil background values. Sc was a trace element, and has no significant anthropogenic sources, so Sc was selected as guideline element³². Generally, according EF value the soils can be classified as six enrichment grades: < 1 (minimal), 1–2 (mild), 2–5 (moderate), 5–20 (significant), 20–40 (very high), and ≥ 40 (extremely high).

Pollution index (PI) and synthetic pollution index (SPI)

For evaluate soil HMs contamination level, PI and SPI were calculated:

$$PI = \frac{C_i}{S_i} \quad (3)$$

$$SPI = \sqrt{\frac{\left(\frac{C_i}{S_i}\right)_{\max} + \left(\frac{C_i}{S_i}\right)_{\text{ave}}}{2}} \quad (4)$$

where PI was element i contamination index, SPI was overall score of each HM to the composite contamination. S_i was the valuation criterion of element i , and the national control thresholds were selected as criterion (Table 1).

Composition	Unit	Min	Max	Mean	S.D	Median	CV (%)	Background values of Sichuan Province ³⁷	Background values of purple soils ³⁷	Purple soil in other area			Threshold Values ^a (5.5 < pH ≤ 6.5)
										Sichuan Nanchong ³⁸	Sichuan Xichang ³⁹	Chongqing ⁴⁰	
As	mg/kg	1.61	42.7	7.77	7.32	5.08	94.3	10.4	9.4	11.09	6.29	7.26	40
Cd	mg/kg	0.038	0.51	0.19	0.11	0.16	56.3	0.079	0.094	0.23	0.08		0.3
Cr	mg/kg	34.8	151	69.5	17.4	66.1	25.1	79	64.8	64.99	92.74	52.8	150
Cu	mg/kg	4.31	108	27.9	16.85	25.4	60.3	31.1	26.3	35.26	20.5	28.8	50
Hg	mg/kg	0.010	0.73	0.077	0.089	0.057	116.5	0.061	0.047	/	0.029	0.036	1.8
Ni	mg/kg	9.60	73.3	30.9	11.0	30.6	35.5	32.6	30.7	38.77	39.48	37.4	70
Pb	mg/kg	15.0	76.0	26.5	7.66	25.9	28.9	30.9	27.7	28.98	25.78	23.5	90
Zn	mg/kg	25.6	121	76.8	19.9	82.1	25.9	86.5	82.8	100.65	89.82	82	200
TC	%	0.12	26.2	1.18	3.04	0.68	258	/	/	/	/	/	/
Corg	%	0.11	13.0	0.90	1.53	0.58	170	1.91	0.75	/	/	/	/
TN	mg/kg	293	2031	830	407	738	49.1	/	/	/	/	/	/
TP	mg/kg	152	922	442	177	405	40.1	/	/	/	/	/	/
TS	mg/kg	57.5	1314	189	174	140	92.0	/	/	/	/	/	/
TK	%	0.98	3.24	1.94	0.50	1.98	25.8	2.02	2.00	/	/	/	/
Sc	mg/kg	5.72	28.1	13.0	3.65	12.9	28.0	12.01	11.65	/	/	/	/
Silt grain	%	9.3	49.7	30.8	9.96	31.2	32.4	/	/	/	/	/	/
Sand grain	%	4.0	83.6	42.5	18.15	43.5	42.7	/	/	/	/	/	/
Clay particle	%	3.3	60.8	26.8	11.60	24.1	43.3	/	/	/	/	/	/

Table 1. Descriptive statistical results of topsoil composition. ^aSoil contamination risk screening values (GB 15,618–2018).

According to PI and SPI values, the soils can be classified into 5 contamination categories: < 0.7 (safety), 0.7–1 (alert), 1–2 (low), 2–3 (moderate) and ≥ 3 (severe)⁴.

Potential ecological risk factor (ER) and Potential ecological risk index (RI)

ER was applied to assess the potential ecological risk of individual soil HM³³, ER was calculated:

$$ER = TR_i \times PI_i \quad (5)$$

where TR_i was the HM (i) toxic-response factor of Hg (40), Cd (30), As (10), Pb (5), Cu (5), Cr (2) and Zn (1)³³, TR of Ni was 5³⁴. PI_i was the HM (i) contamination index. The ER classes can be divided into five potential ecological risk grades: < 40 (low), 40–80 (moderate), 80–160 (considerable), 160–320 (high) and ≥ 320 (very high)³⁵.

RI was a method to evaluate soil multi-element ecological risk. RI was calculated^{33,35}:

$$RI = \sum_{i=1}^n ER = \sum_{i=1}^n (TR_i \times PI_i) \quad (6)$$

where $\sum_{i=1}^n ER$ was the HM (i) potential ecological risk factor, n is the number of HMs. RI classes can be divided into four potential ecological risk grades: < 150 (low), 150–300 (moderate), 300–600 (considerable) and ≥ 600 (very high)³⁵.

Geographical detector (GD)

Factor detector was one of the four methods for GD³⁶, applied to determine spatial differentiation of dependent variables and the ability of their corresponding variables to illustrate the effect of dependent variables, evaluated by the value of q :

$$q = 1 - \frac{\sum_{h=1}^L N_h \sigma_h^2}{N \sigma^2} = 1 - \frac{SSW}{SST} \quad (7)$$

where $h = 1, \dots, L$ was the classification number of the independent variable X , N_h and N were the classification h and the number of units in the whole region, σ_h^2 and σ^2 were the variance of the dependent variable Y in the classification h and the region. SST and SSW represent the total variance of all categories of the independent variable X and the sum variance in the region. The range of q was [0,1]. The larger q value, the greater the impact of the independent variable X on the dependent variable Y .

Factor selection and data processing

Select soil properties (organic carbon (C_{org}), silt content (X_1), total carbon (TC), total potassium (TK), total nitrogen (TN), clay content (X_3), total phosphorus (TP), sand content (X_2) and total sulfur (TS)), topographic factors (altitude (X_4), slope (X_5) and aspect (X_6)), distance factor (distance from railways (X_7), distance from highway (X_8), distance from provincial highway (X_9), distance from county road (X_{10}), distance from rural road (X_{11}), distance from village road (X_{12}), distance from the river (X_{13}), distance from lakes and reservoirs (X_{14}), distance from urban area (X_{15}), distance from the town (X_{16}) and distance from the village (X_{17})), soil texture (X_{18}) and land use type (X_{19}) 25 factors. When using GD to analyze the impacting factors, all independent variables must be converted to type variables and the dependent variable must be a numerical variable. In this research, the natural breakpoint method was applied to classify the impacting factors. Analysis of correlation and descriptive statistical analysis of the data was carried out by SPSS26.0, sampling map and spatial distribution map were drawn by ArcGIS10.8, mapping was completed by Origin2019, and GD was completed by GeoDetector software (<http://www.geodetector.org/>).

Results and discussion

Basic properties of topsoil in study area

HMs contents and physicochemical properties in topsoil of study area were displayed in Table 1. Mean concentrations of TC, Corg, TN, TS, TP and TK were 1.18%, 0.90%, 830 mg/kg, 189 mg/kg, 442 mg/kg and 1.94%, and the mean contents of silt grain, sand grain, clay particle were 30.8%, and 42.5%, and 26.8%.

Average concentrations of Cd, As, Cr, Hg, Cu, Ni, Zn and Pb were 0.19, 7.77, 69.5, 0.077, 27.9, 30.9, 76.8 mg/kg and 26.5 mg/kg. Average contents of Cd and Hg were larger than the Sichuan province soil background values³⁷, compared with purple soil background values³⁷, average contents of Hg, Cd, Cr, Cu and Ni were greater than the values of background. Compared with the risk screening standard value for soil (GB15618-2018), average contents of all HMs were less than the contamination risk screening value, but the maximum As, Cu, Cr, Cd and Ni contents were 1.07, 2.16, 1.01, 1.69 and 1.05 times higher than their corresponding pollution risk screening value. The coefficient of variation was proportional to the degree of interference from external factors such as human activities³², the coefficient of variation of Hg and As were 116.5% and 94.3% in study area indicates that they may be affected by some external interference factors. In comparison with other purple soil areas except that the content of Zn was higher than that of purple soil in Sichuan Nanchong, the contents of other HMs were lower than those in purple soil in Nanchong, Sichuan³⁸. Contamination of Hg, As, Pb, Cd and Cr were greater than their corresponding purple soil values in Sichuan Xichang³⁹, and the contents of As, Cd, Hg, Cu and Pb were larger than respective purple soil values in Chongqing⁴⁰.

Soil HMs spatial distribution features

Figure 2 shows HMs spatial distribution in purple soil of research area. As a whole, soil HMs spatial distribution was significant various from the south to north of this research area. It can be seen that the large value regions of Cu, As, Zn, Hg, Pb, Ni and Cr were mainly distributed in northeast and southwest regions. The hotspots of large Cd distributed in north and northeast areas.

Profile distribution characteristics of soil HMs

The average HMs contents in the purple soil profiles were showed in Fig. 3. The content of Cr was then increased greatly versus depth and minimum value in the surface soil in all profile sampling points. The distribution patterns of Cd and Hg in soil were opposite. For As and Pb, fluctuations changed with increasing soil depths. For Cu, Ni and Zn, at sampling sites of PMC, PMD and PME decreased at first and then increased with the increase of depth, while at sampling sites of PMA and PMB did not change significantly with depth.

Evaluation of environmental risk

The results of I_{geo} , EF, PI and SPI were presented in Fig. 4. The average I_{geo} (Fig. 4a) values followed the descending sequence: $Cd > Hg > Cr > Ni > Cu > Pb > Zn > As$, mean I_{geo} values of other 7 HMs except Cd were < 0 , indicating that purple soil in research area was unpolluted by other HMs, but soils were unpolluted to moderately polluted

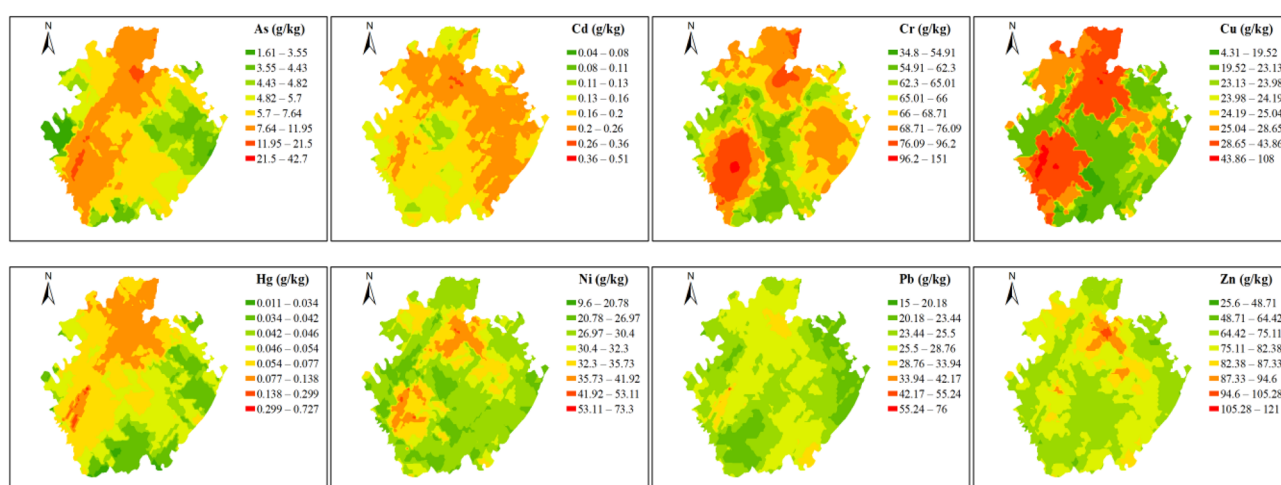


Figure 2. HMs spatial distribution in the topsoil.

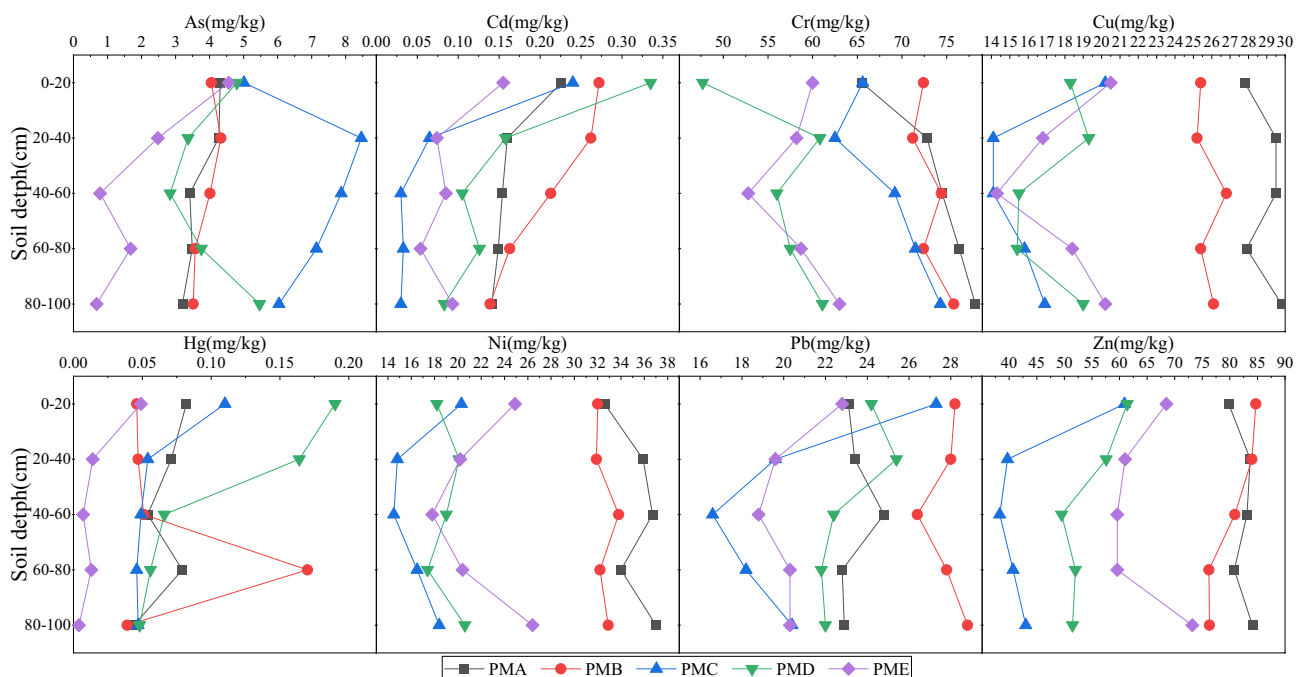


Figure 3. HMs profile distribution in the research region.

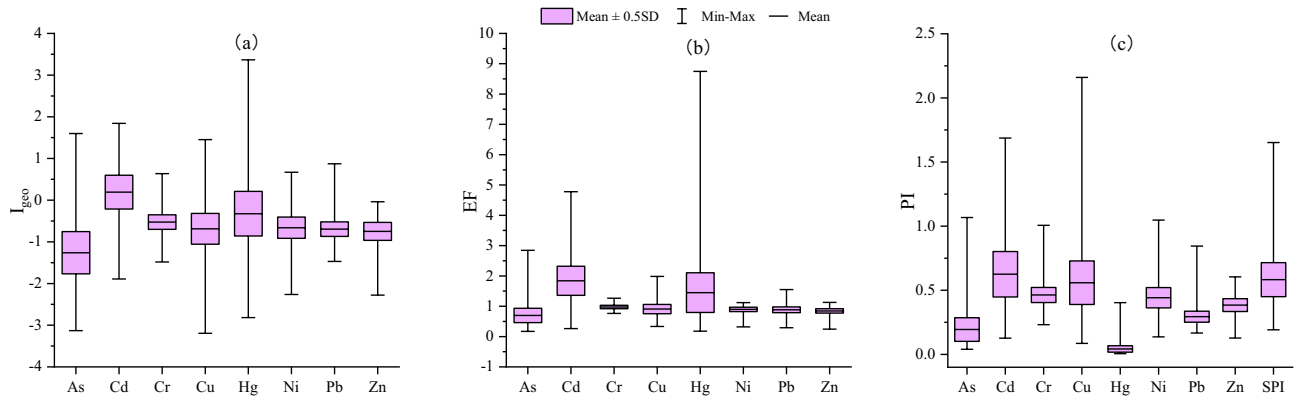


Figure 4. The I_{geo} (a), EF (b), PI (c) and SPI (c) for HMs in purple soils of study area.

by Cd. Among all HMs, Hg and Cd had the greatest mean values of EF ($1 < EF < 2$) (Fig. 4b), meaning that Hg and Cd were mild enrichment in purple soil, the highest EF of Hg and Cd were 8.75 and 4.78. Mean values of EF for other HMs were below 1, showed the minimal enrichment. Although the largest PI (Fig. 4c) values of Cu, Cd, As, Ni, Cr, Pb, Zn and Hg were 2.16, 1.69, 1.07, 1.05, 1.01, 0.84, 0.61 and 0.40, the PI means of all HMs were below than 0.7. It means that research area soil generally has no significant pollution, but there is a phenomenon of point source pollution. The mean SPI values (0.58 ± 0.26) for all HMs, meaning that the soil has no significant pollution with all HMs.

Evaluation of ecological risk

The values of ER and RI were given in Fig. 5. Average ER values followed the descending order: Hg (65.2) > Cd (59.9) > As (8.26) > Cu (5.31) > Ni (5.04) > Pb (4.78) > Cr (2.15) > Zn (0.93), Hg and Cd highest mean ER values ($40 < ER < 80$), meaning that soil Hg and Cd potential ecological risk were moderate, other HMs potential ecological risk were low with mean ER values < 40. The samples with ER values higher than 40 of Cd, Hg and As respective accounted for 65.8%, 58.9% and 2.74%, indicating that Cd and Hg in research area has significant ecological risks, As has certain ecological risks, the ecological risk of other HMs was low. Mean value of RI was 152 and the range of RI values were 51.0 to 868, the samples with RI values higher than 150 accounted for 31.5%, indicating that demonstrating moderate ecological risk in this research. This was similar to the ecological risk estimation results of HMs in Xichang purple soils by Li³⁹.

Multivariate statistical methods

Correlation analysis

Correlation analysis results were displayed in Fig. 6. The results displayed that there was obviously correlation among most HMs, but interestingly, there was no significant correlation among As-Zn and Hg-Zn. Among the influencing factors of soil properties (TC, Corg, TN, TP, TK, TS, Sc, X_1 , X_2 and X_3), 8 HMs were significantly correlated with 6–9 of them, indicating that soil properties had significant effects on all HMs except Ni. Among the topographic factors (X_4 , X_5 and X_6), only As, Cr, Cu, and Ni showed significant positive correlation with X_4 . Among the distance factors (X_7 , X_8 , X_9 , X_{10} , X_{11} , X_{12} , X_{13} , X_{14} , X_{15} , X_{16} and X_{17}), only As showed a significant

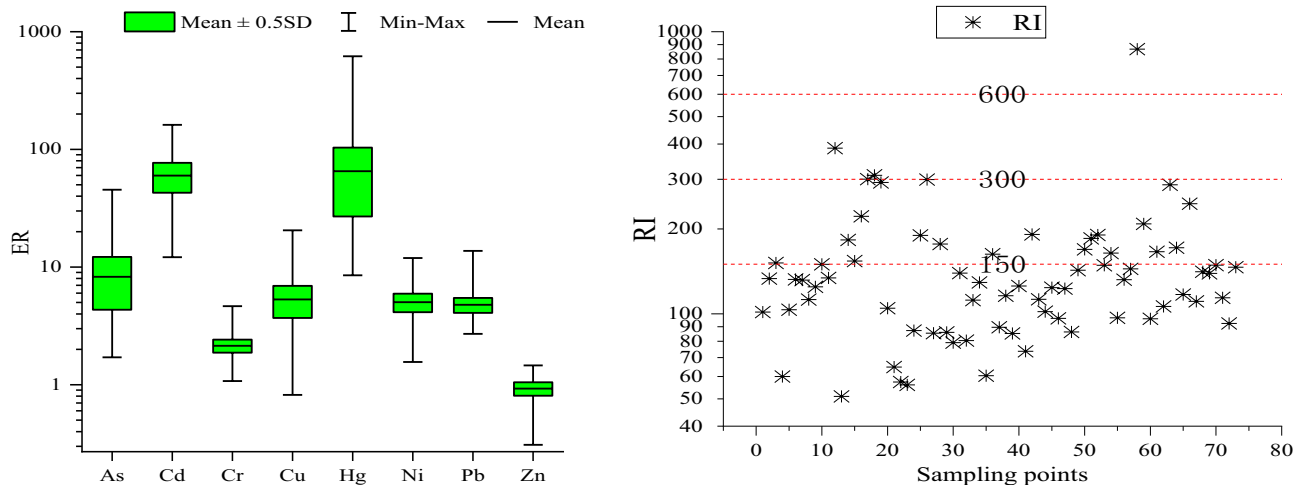


Figure 5. The ER and RI for HMs in soils study area.

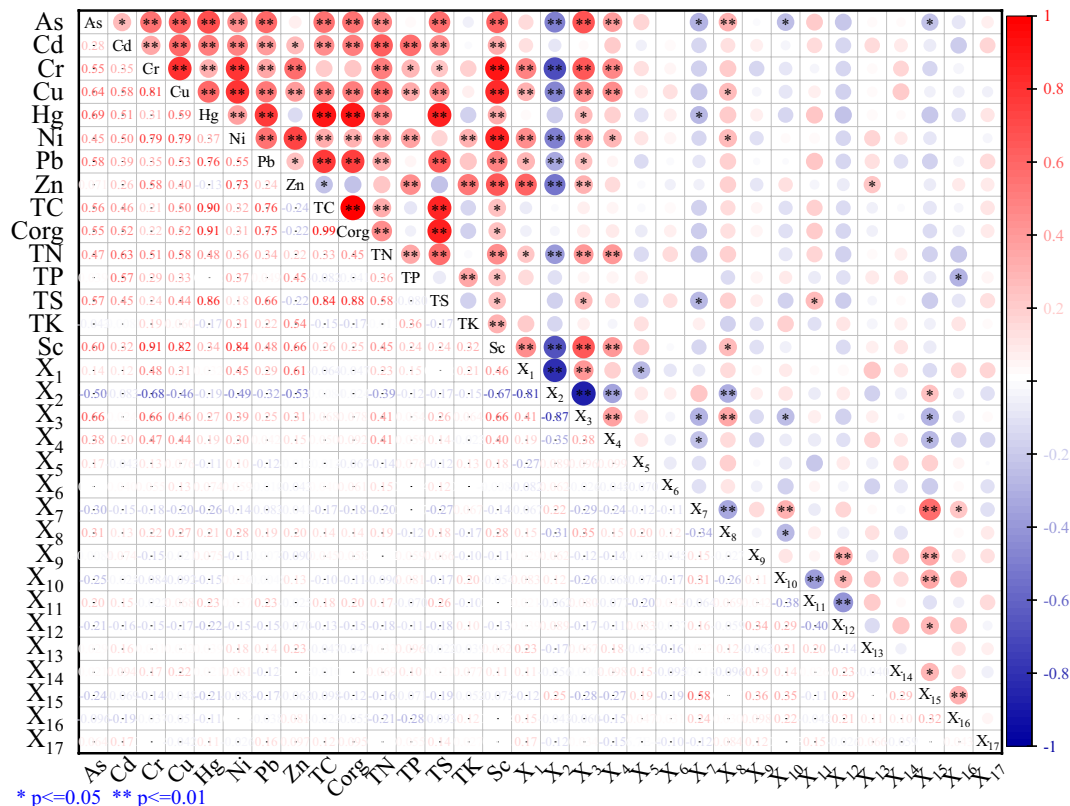


Figure 6. Pearson correlation coefficient of purple soil HMs and impact factors.

positive correlation with X₈, but an obviously negative correlation with X₇, X₁₀ and X₁₅, a obviously negative correlation between Ni and Cu with X₈, and a obviously negative correlation between Hg with X₇. It means that the distance factor has a inevitable effect on HMs in purple soil. Generally, 8 kinds of HMs are greatly affected by natural factors, but they are affected by some external sources, which was consistent with the previous research^{41,42}.

Principal component analysis (PCA)

The PCA results of PTEs in soils were showed in Table 2. The test value p less than 0.0001 of Bartlett’s sphericity and KMO score of 0.753 meaning that the dataset was suitable for PCA. The eigenvalues of two factors (3.19 and 2.89), the cumulative contribution rate was 76.1%, which could basically explain the information contained in the purple soil HMs.

The first principal component (PC1) had strong positive loadings with Hg (0.966), As (0.803), Pb (0.790) and Cd (0.521), and explained 39.9% of the sum variance. According to the results of correlation analysis, there was a very obviously correlation (p < 0.01) between As-Hg, As-Pb, Hg-Cd, Hg-Pb and Pb-Cd, and a significant correlation (p < 0.05) between As with Cd, indicating that the four HMs probably came from the same source, which was consistent with the results of PCA. The mean values of Pb, Hg and Cd were greater than their respective Sichuan Province soil background values and purple soil background values. Although the content of As was less than the value of background, its variation coefficient was as high as 94.3%, indicating that As was disturbed by pollution from external sources that cannot be ignored. Combined with the spatial distribution map (Fig. 2), the great content areas of As, Hg, Pb and Cd are mainly concentrated in southwest and northeast of research region. The central part of study area is a densely populated and traffic-intensive area, which is affected by huge domestic sewage discharge, industrial wastes, motor vehicle exhaust emissions, pesticides and chemical fertilizers and other external pollution sources. We determine PC1 as the source of human activity pollution.

The second principal component (PC2) explained 36.2% variance contribution rate, the strong loadings on Zn (0.912), Ni (0.870), Cr (0.808) and Cu (0.647). Although the contents of Cr, Ni and Cu except Zn were slightly higher than corresponding purple soil background values in China, the four HMs were all less than the

Variable	Hg	As	Pb	Cd	Zn	Ni	Cr	Cu	Eigenvalues	% of variance	Cumulative %
PC1	0.966	0.803	0.790	0.521	- 0.136	0.392	0.361	0.647	3.19	39.9	39.9
PC2	- 0.030	0.198	0.229	0.376	0.912	0.870	0.808	0.647	2.89	36.2	76.1

Table 2. PCA results of HMs in purple soil. Significant values are in [bold].

corresponding Sichuan Province soil background values (Table 1). These four HMs showed a very important positive correlations with each other ($r > 0.58$, $p < 0.01$) except Cu–Zn ($r = 0.40$, $p < 0.01$). Also, these four HMs exhibited lower EF and I_{geo} values. Related studies show that Cr, Zn, Ni and Cu are mainly affected by soil parent materials⁴³. They were mainly controlled by natural sources. PC1 can be judged to be a natural source. It should be noted that Cu also has equal loading on PC1 (0.647), indicating that Cu has the possibility of multiple sources. Previous research on this area pointed out that soil parent material plays an serious role in soil Cu enrichment, and the use of chemical fertilizers affects Cu enrichment to a certain extent⁴⁴.

Influencing factors affecting the spatial heterogeneity of HMs according to GD

The geographical detection results of 25 factors for 8 kinds of HMs were displayed in Fig. 7. There was certain discrepancy in the explanation power of various factors for the 8 HMs, but overall, X_{18} , X_4 , TN, X_3 , X_2 and X_1 have great explanatory power for each HM content spatial distribution. The first impacting factor of As was X_3 (0.450), followed by X_2 (0.240), TS (0.372) and X_{18} (0.360), followed by X_{14} (0.280) and TN (0.236). The first influencing factor of Cd was Corg (0.443), followed by TC (0.422) and TN (0.417), TP (0.299), X_4 (0.189) and TS (0.188) also had significant influence. The first, second and third influencing factors of Cr were X_2 (0.433), X_{18} (0.433) and X_3 (0.403). X_4 (0.399), TN (0.246) and X_1 (0.242) also has great influence. The main influencing factors of Cu were X_4 (0.37) and TN (0.311), and X_2 (0.286), Corg (0.265), X_3 (0.264), TS (0.247), X_{18} (0.243) and TC (0.242) were also important factors impacting the spatial differentiation of Cu content. The first impacting factor of Hg was TS (0.376), followed by Corg (0.326), and TC (0.293), TN (0.274), and X_{18} (0.201) also has significant effects. The primary influencing factor of Ni is X_4 (0.368), followed by X_2 (0.287) and X_{18} (0.253), followed by X_1 (0.184) and X_3 (0.156). The first, second, and third influencing factors of Pb are X_{18} (0.238), X_2 (0.200), and X_4 (0.168). TN (0.16), X_1 (0.158), and Corg (0.158) also has significant effects. The five factors that have the greatest impact on the spatial differentiation of Zn content were X_1 (0.383), X_{18} (0.374), TK (0.334), X_2 (0.326), and TP (0.229).

The ranking of the impact factors on different HMs varies, revealing the heterogeneity of the mechanisms of HM changes. A large area of crops was planted in research area, and feeding, irrigation, and spraying pesticide directly impact soil physical and chemical properties, accompanied by the introduction of HMs⁴⁵. Changes in soil physical and chemical properties directly affect soil HMs activity⁴⁶, migration and transformation⁴⁷. Correlation analysis also showed that TC, Corg, TN, TP, TK, TS, X_1 , X_2 , X_3 and X_{18} were significantly correlated with one or more HMs, so soil physical and chemical properties were important indicators affecting the spatial distribution of HMs. Topographic factors reflect that the soil HMs spatial distribution was affected by natural factors, and the influence process is slow⁴⁸. The altitude (X_4) of research area has a significant impact on 8 HMs spatial distribution, especially on Cu and Ni. Many previous studies have also shown similar conclusions^{49,50}. Interestingly, comparing the Pearson correlation analysis, it was found that there was consistency and difference in the results between Pearson correlation analysis with geographic detection analysis. Consistency, such as the significant relevance between altitude and As, Cr, Cu, and Ni, also has important impact on their spatial distribution; Differences, such as correlation analysis, showed no significant correlation between altitude and Cd, Hg, Pb, and Zn. Geographic detection analysis showed that altitude had a significant impact on the Cd, Hg, Pb, and Zn spatial distribution. It was because GD analyzed the relevance between HMs and impacting factors, containing nonlinear relationships and linear relationships, but coefficient of Pearson correlation was not obviously, meaning that there was no obviously linear relationship between HMs and impacting factors, while it does not mean there was no non-linear relationship⁵¹. The influence of slope (X_5) and aspect (X_6) on HMs was not

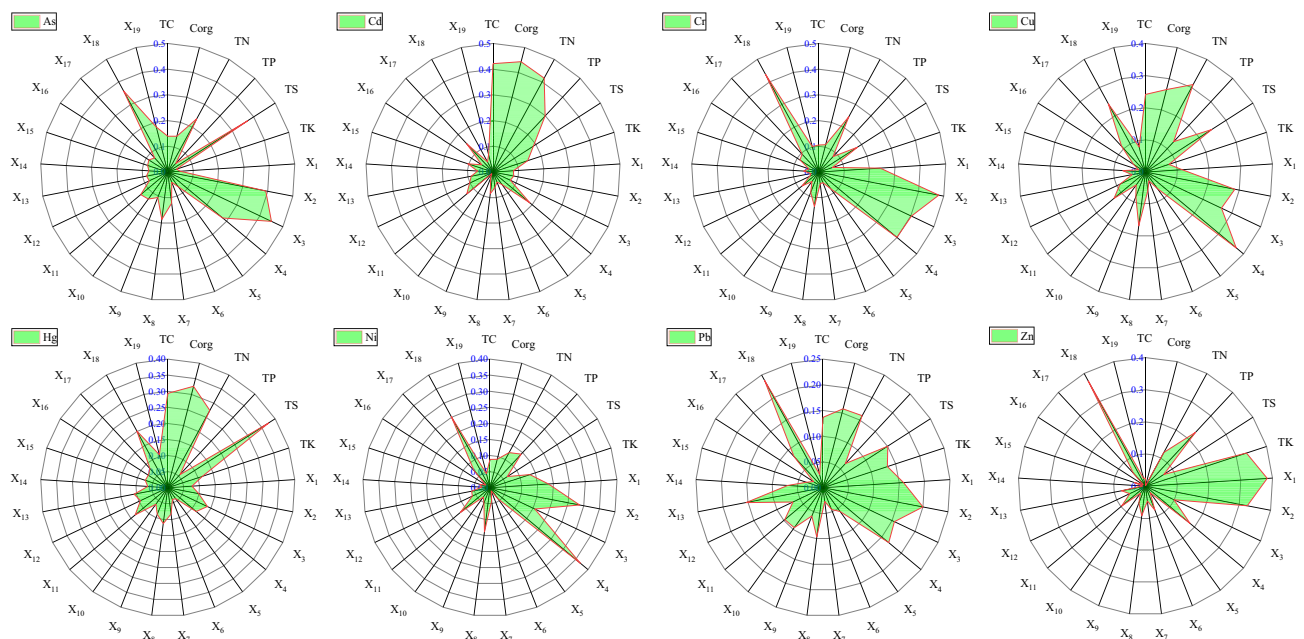


Figure 7. The q value of influencing factors affecting spatial heterogeneity of soil HMs in study area.

obvious, which may be due to the little variation range of aspect and slope in research area. The land use type (X_{19}) only has significant impact on the As, Cr and Hg spatial distribution, but has no significant impact on the other 5 HMs spatial distribution.

Among the 11 distance factors X_7 , X_8 , X_9 , X_{10} , X_{11} , X_{12} , X_{13} , X_{14} , X_{15} , X_{16} and X_{17} , except for X_{14} and X_{16} , all have obvious influence on the spatial distribution of one or more HMs in soil of research region, it was represented in the complex impact of anthropogenic effect about the spatial distribution changes of soil HMs. Anthropogenic activities have shifted natural state of soil HMs distribution characteristics, creating fresh spatial characteristics⁴⁸. Many studies have proved that there was an obvious enrichment of HMs in the soil around roads^{52–54} or railways^{55–57} because the particles containing HMs formed by automobile exhaust emissions and tire wear enter the soil by atmospheric migration and deposition. River system was an significant water source for agricultural irrigation. HMs enrichment in water sources was caused through industrial discharge and transportation, and then farmland soil enrichment was caused through agricultural irrigation^{58–60}. The HMs carried by the “three wastes” from various industries distributed in the study area were enriched in soil by atmospheric deposition, rain water infiltration and erosion. Related researches have displayed residential regions were the most frequent areas of anthropogenic activities, and daily life of residents will generate massive domestic waste containing HMs, which will lead to changes in soil around the residential regions, and the impact will also decrease with the increase of the distance from the residential areas^{61,62}. At the same time, the dense traffic network and frequently anthropogenic activities in towns and cities makes massive pollutants enrich into soil by means of atmospheric deposition and other diffusion ways to produce pollution⁶³.

Conclusions

An integrated approach consists of multivariate statistical analyses, PCA model and GD model is an effective method to identify the ecological risk and sources of HMs in typical purple soil. The average Cd and Hg contents were larger than the Sichuan province soil background values. Mean Cr, Cd, Cu, Ni and Hg contents were larger than the purple soil background values. The ranking of I_{geo} evaluation results was Cd > Hg > Cr > Ni > Cu > Pb > Zn > As, the enrichment sequence of HMs in purple soil was Cd > Hg > Cr > Cu > Ni > Pb > Zn > As, the contamination sequence was Cd > Cu > Cr > Ni > Zn > Pb > As > Hg and the comprehensive pollution factor results show that there was no significant pollution of HMs in the soil of the research region. The sequence of potential ecological risks was Hg > Cd > As > Cu > Ni > Pb > Cr > Zn. Cd and Hg have the highest potential ecological risks and were at a higher risk level. PCA analysis show that Hg, As, Pb and Cd come from human activities, but Ni, Zn and Cr mainly come from natural sources, while Cu was affected by both natural sources and human activities. Geographical exploration analysis showed that, among the 25 influencing factors, X_{18} , X_4 , TN, X_3 , X_2 and X_1 had the strongest explanatory power to explain the spatial differentiation of 8 HMs. This study provides useful information for determining the distribution characteristics, possible sources, and environmental risks of HM pollution in typical purple soil, which will help to develop targeted policies and measures to reduce HM pollution in purple soil environments.

Data availability

The authors declare that all data supporting the findings of this study are available within the article.

Received: 2 January 2024; Accepted: 15 April 2024

Published online: 18 May 2024

References

1. Tepanosyan, G., Sahakyan, L., Belyaeva, O., Asmaryan, S. & Saghatelian, A. Continuous impact of mining activities on soil heavy metals levels and human health. *Sci. Total Environ.* **639**, 900–909 (2018).
2. Ding, Q., Cheng, G., Wang, Y. & Zhuang, D. Effects of natural factors on the spatial distribution of heavy metals in soils surrounding mining regions. *Sci. Total Environ.* **578**, 577–585 (2017).
3. Niu, L., Yang, F., Xu, C., Yang, H. & Liu, W. Status of metal accumulation in farmland soils across China: From distribution to risk assessment. *Environ. Pollut.* **176**, 55–62 (2013).
4. Gong, C. *et al.* Spatial distribution characteristics of heavy metal(loid)s health risk in soil at scale on town level. *Sci. Rep.* <https://doi.org/10.1038/s41598-022-20867-4> (2022).
5. Karimyan, K. *et al.* Human health and ecological risk assessment of heavy metal(loid)s in agricultural soils of rural areas: A case study in Kurdistan Province Iran. *J. Environ. Health Sci. Eng.* **18**, 469–481. <https://doi.org/10.1007/s40201-020-00475-y> (2020).
6. Yang, Q. Q. *et al.* A review of soil heavy metal pollution from industrial and agricultural regions in China: Pollution and risk assessment. *Sci. Total Environ.* **642**, 690–700. <https://doi.org/10.1016/j.scitotenv.2018.06.068> (2018).
7. Huang, Y. *et al.* Heavy metal pollution and health risk assessment of agricultural soils in a typical peri-urban area in southeast China. *J. Environ. Manage.* **207**, 159–168. <https://doi.org/10.1016/j.jenvman.2017.10.072> (2018).
8. Li, Z. X. *et al.* Effect and hazard of common metal elements on human body. *Mater. China* **39**, 934–944. <https://doi.org/10.7502/j.issn.1674-3962.202003018> (2020).
9. Zhang, C. L. *et al.* Sources of heavy metal pollution and risk assessment of soil in watermelon planting areas in Kaifeng City. *Environ. Chem.* **40**, 1714–1722. <https://doi.org/10.7524/j.issn.0254-6108.2020013002> (2021).
10. De Temmerman, L., Vanongeval, L., Boon, W., Hoenig, M. & Geypens, M. Heavy metal content of arable soils in Northern Belgium. *Water, Air, Soil Pollut.* **148**, 61–76. <https://doi.org/10.1023/a:1025498629671> (2003).
11. Li, P., Huang, Y., Lin, Y., Hua, P. X. & Yuan, G. L. Distribution, source identification and risk assessment of heavy metals in topsoil of huairou district in Beijing. *Geoscience* **32**, 86–94. <https://doi.org/10.19657/j.geoscience.1000-8527.2018.01.08> (2018).
12. Xiao, Y. *et al.* Spatial distribution, pollution, and health risk assessment of heavy metal in agricultural surface soil for the Guangzhou-Foshan urban zone South China. *Plos One* **15**, 1–17. <https://doi.org/10.1371/journal.pone.0239563> (2020).
13. Xiaoi, D. *et al.* Spatial-temporal pattern evolution and driving force analysis of ecological environment vulnerability in Panzhuhai City. *Environ. Sci. Pollut. Res. Int.* **28**, 7151–7166 (2020).
14. Yang, A., Wang, Y., Hu, J., Liu, X. & Li, J. Evaluation and source of heavy metal pollution in surface soil of Qinghai-Tibet plateau. *Environ. Sci.* **41**, 886–894. <https://doi.org/10.13227/j.hjcx.201907195> (2020).

15. Bo, L. J. *et al.* Characteristics and potential ecological risk assessment of heavy metals in garlic producing areas of Jinxiang. *Chinese J. Soil Sci.* **52**, 434–442. <https://doi.org/10.19336/j.cnki.trtb.2020061601> (2021).
16. Guo, Z. *et al.* Characteristics of soil heavy metal pollution and health risk in Xiongan New District. *China Environ. Sci.* **41**, 431–441. <https://doi.org/10.19674/j.cnki.issn1000-6923.2021.0049> (2021).
17. Liu, H. W. *et al.* Quantitative source apportionment, risk assessment and distribution of heavy metals in agricultural soils from southern Shandong Peninsula of China. *Sci. Total Environ.* **767**, 144879. <https://doi.org/10.1016/j.scitotenv.2020.144879> (2021).
18. Liu, P. *et al.* Accumulation and ecological risk of heavy metals in soils along the coastal areas of the Bohai Sea and the Yellow Sea: A comparative study of China and South Korea. *Environ. Int.* <https://doi.org/10.1016/j.envint.2020.105519> (2020).
19. Dong, B. *et al.* Multiple methods for the identification of heavy metal sources in cropland soils from a resource-based region. *Sci. Total Environ.* **651**, 3127–3138. <https://doi.org/10.1016/j.scitotenv.2018.10.130> (2019).
20. Chai, Y. *et al.* Source identification of eight heavy metals in grassland soils by multivariate analysis from the Baicheng-Songyuan area, Jilin Province Northeast China. *Chemosphere* **134**, 67–75. <https://doi.org/10.1016/j.chemosphere.2015.04.008> (2015).
21. Liu, H. W. *et al.* Quantitative source apportionment, risk assessment and distribution of heavy metals in agricultural soils from southern Shandong Peninsula of China. *Sci. Total Environ.* <https://doi.org/10.1016/j.scitotenv.2020.144879> (2021).
22. Gong, C. *et al.* Spatial differentiation and influencing factor analysis of soil heavy metal content at town level based on geographic detector. *Environ. Sci.* **43**, 4566–4577. <https://doi.org/10.13227/j.hjcx.202112077> (2022).
23. Gong, C. *et al.* Ecological and human health risk assessment of heavy metal(loid)s in agricultural soil in hotbed chives hometown of Tangchang Southwest China. *Sci. Rep.* <https://doi.org/10.1038/s41598-022-11397-0> (2022).
24. Nanos, N. & Martín, J. A. R. Multiscale analysis of heavy metal contents in soils: Spatial variability in the Duero river basin (Spain). *Geoderma* **189**, 554–562. <https://doi.org/10.1016/j.geoderma.2012.06.006> (2012).
25. Ren, Z. Q., Xiao, R., Zhang, Z. H., Lv, X. N. & Fei, X. F. Risk assessment and source identification of heavy metals in agricultural soil: A case study in the coastal city of Zhejiang Province, China. *Stochastic Environ. Res. Risk Assess.* **33**, 2109–2118. <https://doi.org/10.1007/s00477-019-01741-8> (2019).
26. Zheng, S. N., Chen, C., Li, Y. N., Li, S. & Liang, J. F. Characterizing the release of cadmium from 13 purple soils by batch leaching tests. *Chemosphere* **91**, 1502–1507. <https://doi.org/10.1016/j.chemosphere.2012.12.026> (2013).
27. Qilin, L., Chaofu, W., Yun, H., Liwei, W. & Dingyong, W. A study on the characteristics of heavy metals in orange ecosystem. *Chinese J. Geochem.* **29**, 100–106 (2010).
28. Wu, F. Z., Yang, W. Q., Zhang, J. & Zhou, L. Q. Cadmium accumulation and growth responses of a poplar (*Populus deltoids* x *Populus nigra*) in cadmium contaminated purple soil and alluvial soil. *J. Hazardous Mater.* **177**, 268–273. <https://doi.org/10.1016/j.jhazmat.2009.12.028> (2010).
29. Du, J., Wang, Z. K., Liu, J., Zhong, S. Q. & Wei, C. F. Distribution characteristics of soil heavy metals, their source identification and their changes influenced by anthropogenic cultivation activities in purple hilly regions of Sichuan basin, China. *J. Soil Sci. Plant Nutr.* **20**, 1080–1091. <https://doi.org/10.1007/s42729-020-00194-1> (2020).
30. Ministry of Land and Resources of the People's Republic of China. DZ/T 0295–2016 Specification of land quality geochemical assessment (2016).
31. Qiao, P. W., Yang, S. C., Lei, M., Chen, T. B. & Dong, N. Quantitative analysis of the factors influencing spatial distribution of soil heavy metals based on geographical detector. *Sci. Total Environ.* **664**, 392–413. <https://doi.org/10.1016/j.scitotenv.2019.01.310> (2019).
32. Zhang, Z. S., Zheng, D. M., Xue, Z. S., Wu, H. T. & Jiang, M. Identification of anthropogenic contributions to heavy metals in wetland soils of the Karuola Glacier in the Qinghai-Tibetan Plateau. *Ecol. Indic.* **98**, 678–685. <https://doi.org/10.1016/j.ecolind.2018.11.052> (2019).
33. Hakanson, L. An ecological risk index for aquatic pollution control A sedimentological approach. *Water Res.* **14**(8), 975–1001 (1980).
34. Xu, Z. Q., Ni, S. J., Tuo, X. G. & Zhang, C. J. Calculation of heavy metals' toxicity coefficient in the evaluation of potential ecological risk index. *Environ. Sci. Technol.* **31**, 112–115. <https://doi.org/10.19672/j.cnki.1003-6504.2008.02.030> (2008).
35. Varol, M., Sunbul, M. R., Aytol, H. & Yilmaz, C. H. Environmental, ecological and health risks of trace elements, and their sources in soils of Harran Plain Turkey. *Chemosphere* <https://doi.org/10.1016/j.chemosphere.2019.125592> (2020).
36. Wang, J. F. *et al.* Geographical detectors-based health risk assessment and its application in the neural tube defects study of the Heshun Region, China. *Int. J. Geograph. Inform. Sci.* **24**, 107–127. <https://doi.org/10.1080/13658810802443457> (2010).
37. *Element Background Values of China Soils*. China National Environmental Monitoring Center edn, (China Environment Publishing Group, 1990).
38. Zhou, R. Y., Wang, D., Wen, M. & Wen, X. Y. Response of magnetic susceptibility and particle size to heavy metal pollution for the purple soil in the Jialing river basin China. *J. Sichuan Agric. Univ.* **41**, 683–689. <https://doi.org/10.16036/j.issn.1000-2650.202103199> (2023).
39. Li, T. *et al.* Migration and enrichment characteristics of heavy metals in purple soil of a profile in the Pushi clastic rock area, Xichang region, Sichuan, China and their ecological risk assessment. *Acta Mineral. Sinica* **43**, 125–136. <https://doi.org/10.16461/j.cnki.1000-4734.2022.42.079> (2023).
40. Yin, Q. H. *et al.* Geochemical background values of some trace elements in purple soil in Chongqing. *J. Southwest Teachers College*, 45–53, doi:<https://doi.org/10.13718/j.cnki.xsxb.1985.03.006> (1985)
41. Liu, Y. R., He, Z. Y., Yang, Z. M., Sun, G. X. & He, J. Z. Variability of heavy metal content in soils of typical Tibetan grasslands. *Rsc Adv.* **6**, 105398–105405. <https://doi.org/10.1039/c6ra23868h> (2016).
42. Sheng, J. J., Wang, X. P., Gong, P., Tian, L. D. & Yao, T. D. Heavy metals of the Tibetan top soils Level, source, spatial distribution, temporal variation and risk assessment. *Environ. Sci. Pollut. Res.* **19**, 3362–3370. <https://doi.org/10.1007/s11356-012-0857-5> (2012).
43. Chen, M., Pan, Y. X., Huang, Y. X., Wang, X. T. & Zhang, R. D. Spatial distribution and sources of heavy metals in soil of a typical lead-zinc mining area, Yangshuo. *Environ. Sci.* **43**(10), 4545–4555 (2022).
44. Wang, C. *Soil copper enrichment mechanism and land use zoning in Linshui county* (Sichuan province, China University of Geosciences (Beijing), 2022).
45. Wei, Z. M. *et al.* Pollution characteristics and risk assessment of heavy metals in farmland soils at Shizhuyuan Donghe River basin of Southern Hunan. *Environ. Chem.* **39**, 2753–2764. <https://doi.org/10.7524/j.issn.0254-6108.2019073103> (2020).
46. Lazar, G. C. B., Stătescu, F. & Toma, D. Study of heavy metal dynamics in soil. *Environ. Eng. Manag. J.* **19**, 359–367 (2020).
47. Qian, J., Shana, X. Q., Wang, Z. J. & Tu, Q. Distribution and plant availability of heavy metals in different particle-size fractions of soil. *Sci. Total Environ.* **187**, 131–141. [https://doi.org/10.1016/0048-9697\(96\)05134-0](https://doi.org/10.1016/0048-9697(96)05134-0) (1996).
48. Song, H. F. & WU KN, L. I. The spatial distribution and influencing factors of farmland heavy metals in the cold black soil region: A case of Hailun county. *Chinese J. Soil Sci.* **49**(6), 1480–1486 (2018).
49. Qin, Y. L., Zhang, F. G., Xue, S. D., Ma, T. & Yu, L. S. Heavy metal pollution and source contributions in agricultural soils developed from Karst landform in the southwestern region of China. *Toxics* <https://doi.org/10.3390/toxics10100568> (2022).
50. Li, S. J., Yang, L., Chen, L. D., Zhao, F. K. & Sun, L. Spatial distribution of heavy metal concentrations in peri-urban soils in eastern China. *Environ. Sci. Pollut. Res.* **26**, 1615–1627. <https://doi.org/10.1007/s11356-018-3691-6> (2019).
51. Gong, C. *et al.* Spatial differentiation and influencing factors analysis of soil heavy metal content at scale on town level based on geographic detector. *Environ. Sci.* **43**, 4566–4577. <https://doi.org/10.13227/j.hjcx.202112077> (2022).

52. Zhang, H., Wang, Z. F., Zhang, Y. L. & Hu, Z. J. The effects of the Qinghai-Tibet railway on heavy metals enrichment in soils. *Sci. Total Environ.* **439**, 240–248. <https://doi.org/10.1016/j.scitotenv.2012.09.027> (2012).
53. Liu, H. *et al.* Heavy metal contamination in soil alongside mountain railway in Sichuan China. *Environ. Monit. Assess.* **152**, 25–33. <https://doi.org/10.1007/s10661-008-0293-7> (2009).
54. Stojic, N., Pucarevic, M. & Stojic, G. Railway transportation as a source of soil pollution. *Transp. Res. Part D-Trans. Environ.* **57**, 124–129. <https://doi.org/10.1016/j.trd.2017.09.024> (2017).
55. Bai, J. H., Cui, B. S., Wang, Q. G., Gao, H. F. & Ding, Q. Y. Assessment of heavy metal contamination of roadside soils in Southwest China. *Stochastic Environ. Res. Risk Assess.* **23**, 341–347. <https://doi.org/10.1007/s00477-008-0219-5> (2009).
56. Abderrahmane, B., Naima, B., Tarek, M. & Abdelghani, M. Influence of highway traffic on contamination of roadside soil with heavy metals. *Civil Eng. J. Tehran* **7**, 1459–1471. <https://doi.org/10.28991/cej-2021-03091736> (2021).
57. Wei, B. G. & Yang, L. S. A review of heavy metal contaminations in urban soils, urban road dusts and agricultural soils from China. *Microchem. J.* **94**, 99–107. <https://doi.org/10.1016/j.microc.2009.09.014> (2010).
58. Zhang, K., Su, F. L., Liu, X. M., Song, Z. & Feng, X. Heavy metal concentrations in water and soil along the Hun River, Liaoning, China. *Bull. Environ. Contam. Toxicol.* **99**, 391–398. <https://doi.org/10.1007/s00128-017-2142-2> (2017).
59. Singh, G., Patel, N., Jindal, T. & Ranjan, M. R. Heavy metal contamination in soils and crops irrigated by kali river in Uttar Pradesh, India. *Bull. Environ. Contam. Toxicol.* **107**, 931–937. <https://doi.org/10.1007/s00128-021-03349-7> (2021).
60. Zhao, R. D., Coles, N. & Wu, J. P. Status of heavy metals in soils following long-term river sediment application in plain river network region, southern China. *J. Soils Sediments* **15**, 2285–2292. <https://doi.org/10.1007/s11368-015-1157-8> (2015).
61. Peng, C., Zhang, K., Wang, M. E., Wan, X. X. & Chen, W. P. Estimation of the accumulation rates and health risks of heavy metals in residential soils of three metropolitan cities in China. *J. Environ. Sci.* **115**, 149–161. <https://doi.org/10.1016/j.jes.2021.07.008> (2022).
62. Ashaiekh, M. A. *et al.* Spatial distribution of total and bioavailable heavy metal contents in soil from agricultural, residential, and industrial areas in Sudan. *Toxin Rev.* **38**, 93–105. <https://doi.org/10.1080/15569543.2017.1419491> (2019).
63. Cai, L. M., Wang, Q. S., Wen, H. H., Luo, J. & Wang, S. Heavy metals in agricultural soils from a typical township in Guangdong Province, China: Occurrences and spatial distribution. *Ecotox. Environ. Safe.* **168**, 184–191. <https://doi.org/10.1016/j.ecoenv.2018.10.092> (2019).

Author contributions

Cang Gong: Methodology, Calculation, Writing Original draft, Sample Analysis, Investigation. Wenbin Chen and Guanglong Tian: Sample Collection and Investigation. Wei Zhang and Fei Xiao: Revising the Original draft, Supervision. Licheng Quan and Zhixiang Zhang: Conceptualization, Revising the Original draft, Validation, Supervision.

Funding

This research was supported by Geological Survey Project of China Geological Survey (DD20243098 and ZD20220119) and Open Foundation of the Key Laboratory of Natural Resource Coupling Process and Effects (No.2023KFKTB011).

Competing interests

The authors declare no competing interests.

Additional information

Correspondence and requests for materials should be addressed to L.Q. or Z.Z.

Reprints and permissions information is available at www.nature.com/reprints.

Publisher's note Springer Nature remains neutral with regard to jurisdictional claims in published maps and institutional affiliations.



Open Access This article is licensed under a Creative Commons Attribution 4.0 International License, which permits use, sharing, adaptation, distribution and reproduction in any medium or format, as long as you give appropriate credit to the original author(s) and the source, provide a link to the Creative Commons licence, and indicate if changes were made. The images or other third party material in this article are included in the article's Creative Commons licence, unless indicated otherwise in a credit line to the material. If material is not included in the article's Creative Commons licence and your intended use is not permitted by statutory regulation or exceeds the permitted use, you will need to obtain permission directly from the copyright holder. To view a copy of this licence, visit <http://creativecommons.org/licenses/by/4.0/>.

© The Author(s) 2024